Rovibrational-specific QCT and master equation analysis on the CNO system for high-energy collisions

C. H. B. Civrais[1], B. R. L. Galvão[2], S. M. Jo[3], M. Panesi[1]

[1]Department of Mechanical and Aerospace Engineering, University of California Irvine, Irvine, USA
[2]Centro Federal de Educação Tecnológica de Minas Gerais, Belo Horizonte, Minas Gerais, Brazil
[3]Korea Advanced Institute of Science and Technology, Republic of Korea

Thermal & Fluids Analysis Workshop 2025
NASA Ames Research Center
San Jose, CA
August 4-7, 2025

Outline

Motivation (I)

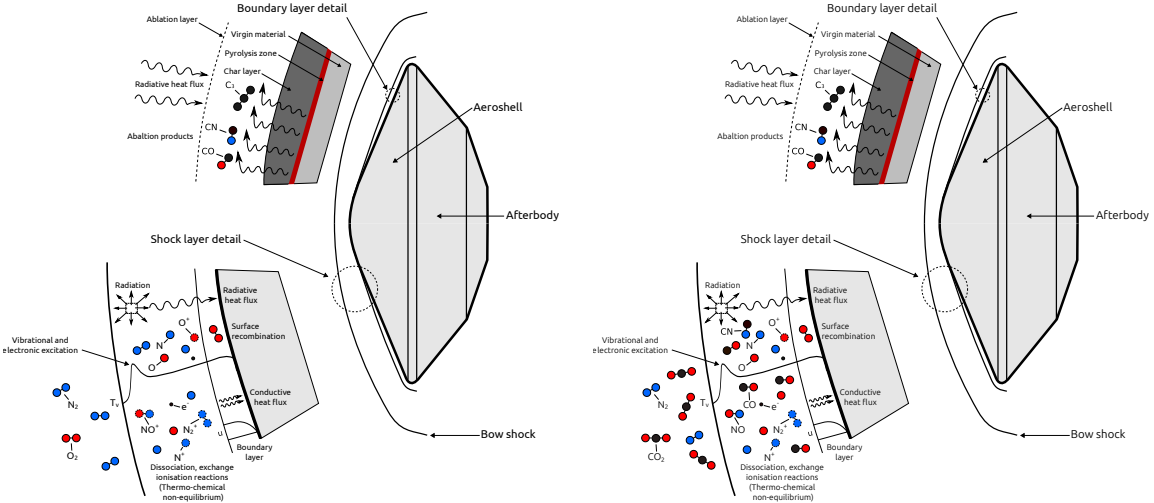

(a) Earth reentry.

(b) Mars and Venus reentry.

Figure: Schematic of the aerothermodynamic processes for Mars and Venus atmospheric entries (adapted from Potter (2011)).

Motivation (II)

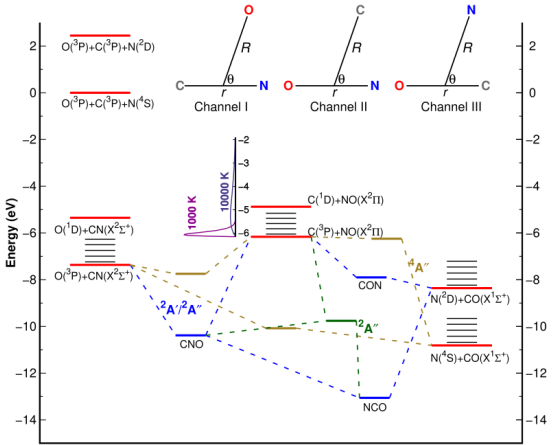

Figure: Schematic of the energy profile for the CNO system (extracted from Koner *et al.* (2018)).

Literature Overview

Table: Experimental calculations of the CNO reaction rates.

Reference	Rate ($cm^3.molecule^{-1}.s^{-1}$)	Temperature (K)
$NO + C \longrightarrow$ Products		
Braun *et al* (1969)	11×10^{-11}	300
Husain and Kirsch (1971)	$7.3 \pm 2.2 \times 10^{-11}$	300
Husain and Young (1974)	$4.8 \pm 0.8 \times 10^{-11}$	300
Becker *et al* (1988)	$1.6 \pm 0.2 \times 10^{-11}$	300
Lindackers *et al* (1990)	$3.3 \pm 0.7 \times 10^{-11}$	2720-3810
Dean *et al* (1991)	$8.0 \pm 3.6 \times 10^{-11}$	1550-4050
Dorthe *et al* (1991)	$2.7 \pm 0.3 \times 10^{-11}$	300
Bergeat *et al* (1999)	$5.4 \pm 0.8 \times 10^{-11}$	300
Chastaing *et al* (2000)	$[22.8 \pm 1.7; 12.0 \pm 0.1] \times 10^{-11}$	15-295
$CN + O \longrightarrow CO + N$		
Boden and Thrush (1968)	$(10.5 \pm 5.8) e^{-\frac{1200 \pm 3500}{T}} \times 10^{-11}$	570-687
Schmatjo and Wolfrum (1978)	$1.7 \pm 0.7 \times 10^{-11}$	298
Louge and Hanson (1984)	$3.0(+2.6/-1.3)10^{-11}$	2000
Davidson *et al* (1991)	$13.0 \pm 2.6 \times 10^{-11}$	3000-4500
Titarchuk and Halpern (1995)	$3.69 \pm 0.75 \times 10^{-11}$	298

Table: Theoretical calculations of the CNO reaction rates.

Reference	Rate ($cm^3.molecule^{-1}.s^{-1}$)	Temperature (K)
$NO + C \longrightarrow CN + O$		
Simonson *et al* (1995)	$2.19\ 10^{-9}\ T^{-0.5} e^{-\frac{0.024}{kT}}$	200-4500
Andersson *et al* (1999)	see article	200-4500
Andersson *et al* (2003)	$5.572\ T^{-0.0315}$	200-5000
Koner *et al* (2018)†	$8.51\ 10^{-11} e^{-\frac{4312}{T}}$	5000-20,000
Koner *et al* (2018)††	$8.66\ 10^{-11} e^{-\frac{4782}{T}}$	5000-20,000
Galvão *et al* (2018-2023)	see article	100-10,000
$NO + C \longrightarrow CO + N$		
Andersson *et al* (1999)	see article	200-4500
Andersson *et al* (2003)	$3.488\ T^{-0.0153}$	200-5000
Koner *et al* (2018)†	$1.46\ 10^{-10} e^{-\frac{5876}{T}}$	5000-20,000
Koner *et al* (2018)††	$1.34\ 10^{-10} e^{-\frac{4195}{T}}$	5000-20,000
Galvão *et al* (2018-2023)	see article	100-10,000
$CN + O \longrightarrow CO + N$		
Andersson *et al* (2003)	$14.512\ T^{-0.178}$	200-5000
Lu *et al* (2024)	see article	100-10,000

†: Adiabatic, and †† : TSH.

Objective

- Gain physical understanding of the energy transfer and reactive mechanisms in the NO + C collisional system.

Approach

- Compute rovibrational state-specific reaction rate coefficients using QCT calculations on *ab initio* potential energy surfaces,
- Conduct 0D isothermal heat bath studies to investigate chemical kinetic processes on the microscopic scale and compute macroscopic quantities of interests, e.g. QSS rate coefficient.

Outline

Computational Workflow and Governing Equations

- Construction of *ab initio* potential energy surface (PES) to characterise the interaction between colliding particles. **Governing equation:** electronic Schrödinger equation, i.e. $\hat{H}_e \Psi_e(\mathbf{r};\mathbf{R}) = E_e(\mathbf{R})\Psi_e(\mathbf{r};\mathbf{R})$,
- Calculation of the cross-section and rate coefficients based on the quasiclassical trajectory (QCT) method. **Governing equations:** Hamilton's equations, i.e.

$$\begin{cases} \dot{q} = \frac{\partial H}{\partial p} \\ \dot{p} = -\frac{\partial H}{\partial q} \end{cases} ,$$

- Determination of the quasi steady state (QSS) rate coefficients by means of master equation analysis. **Governing equations:** set of master equations, i.e. $\frac{\partial n_c^i}{\partial t} = \omega_c^i$.

Potential Energy Surfaces

Table: Overview of the PESs available in the literature.

State	Fitting	*ab initio* energies	Methods	Reference
		Andersson and coworkers		
$^2A'$	MBE*	1029	CASPT2**	Andersson *et al.* (2000)
$^2A''$	MBE	998	CASPT2	Andersson *et al.* (2000)
$^4A''$	MBE	4947	CASPT2	Abrahamsson *et al.* (2008)
		Koner and coworkers		
$^2A'$	RKHS†	≈5,000	MRCI/aug-cc-pVTZ††	Koner *et al.* (2018)
$^2A''$	RKHS	≈5,000	MRCI/aug-cc-pVTZ	Koner *et al.* (2018)
$^4A''$	RKHS	≈5,000	MRCI/aug-cc-pVTZ	Koner *et al.* (2018)
		Galvão and coworkers		
$^2A'$	DMBE‡	3701	MRCI-F12/cc-pVTZ-F12	Gonçalves *et al.* (2018)
$^2A''$	DMBE	5604	MRCI-F12/cc-pVTZ-F12	Alves *et al.* (2021)
$^4A''$	DMBE	3337	MRCI-F12/cc-pVTZ-F12	Alves *et al.* (2023)

*Many body expansion.

**Complete active space second-order perturbation theory.

†Reproducing kernel Hilbert space.

††Multi-reference configuration interaction level of theory including the Davidson correction with the augmented Dunning type correlation consistent polarized triple zeta.

‡Double many body expansion.

Rovibrational-specific Kinetics Database (1)

- Rovibrational excitation and de-excitation through inelastic and homogenous exchange reactions,

$$\mathrm{NO(i)} + \mathrm{C} \underset{k^{I,NO}_{j\to i}}{\overset{k^{I,NO}_{i\to j}}{\rightleftharpoons}} \mathrm{NO(j)} + \mathrm{C} \qquad \text{(Reaction 1)}$$

- Rovibrational energy transfer through the heterogenous exchange reactions,

$$\mathrm{NO(i)} + \mathrm{C} \underset{k^{E,CN}_{m\to i}}{\overset{k^{E,NO}_{i\to m}}{\rightleftharpoons}} \mathrm{CN(m)} + \mathrm{O} \qquad \text{(Reaction 2)}$$

$$\mathrm{NO(i)} + \mathrm{C} \underset{k^{E,CO}_{l,k\to i}}{\overset{k^{E,NO}_{i\to l,k}}{\rightleftharpoons}} \mathrm{CO(l)} + \mathrm{N(k)} \qquad \text{(Reaction 3)}$$

- Rovibrational dissociation and recombination reactions of bound and quasi-bound states,

$$\mathrm{NO(i)} + \mathrm{C} \underset{k^{R}_{c\to i}}{\overset{k^{D,NO}_{i\to c}}{\rightleftharpoons}} \mathrm{N} + \mathrm{O} + \mathrm{C} \qquad \text{(Reaction 4)}$$

Methodology

- QCT calculations are performed with CoarseAIR - modernised version of the VVTC developed at NASA Ames Research Center by David Schwenke,
- Trajectories are integrated separately on each PES: $^2A'$, $^2A''$, and $^4A''$ [a].
- Initial conditions:
  - Sampled from a Boltzmann distribution at T = 7500, 10000, and 20,000 K,
  - Particles initialized with a separation of 30 Bohr between reactants,
  - Impact parameter sampled using 7 circle strata with $b_{max} = 14$ Bohr,
- 10,000 trajectories are performed for each rovibrational state and initial condition,
- Trajectories are terminated if:
  - Separation between colliding partners exceeds 30 Bohr,
  - Trajectory time exceeds 10^5 atomic units.

[a] Doublet PESs lead to the formation of N(^{2}D) whereas the quartet PES leads to the formation of N(^{4}S)

Rovibrational-specific Kinetics Database (3)

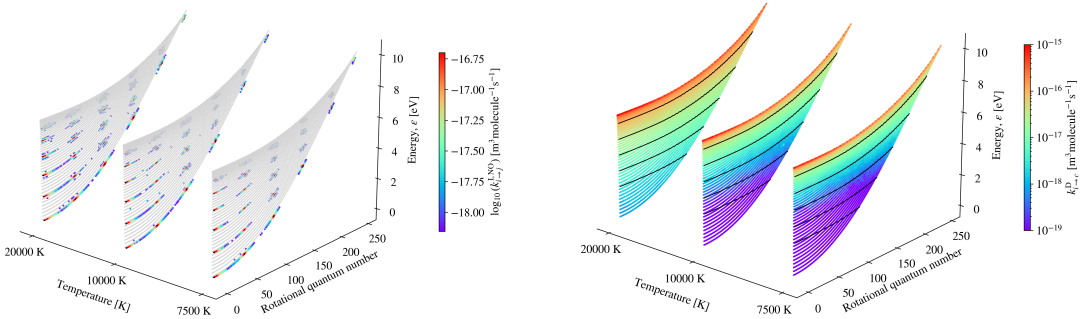

(a) Energy-transfer state-specific rate coefficients $(\mathrm{NO(i)+C \longrightarrow NO(j)+C})$.

(b) Dissociation state-specific rate coefficients $(\mathrm{NO(i)+C \longrightarrow N+O+C})$.

Figure: Distribution of the energy-transfer (left) and total dissociation (right) rate coefficients at T = 10,000 K overlayed on the NO diatomic potential. The black lines denotes the isolines of energy deficit, i.e. distance from the centrifugal barrier.

Master Equation Analysis

Investigate the kinetics processes of NO + C collisional system in term of state population through a set of master equations to extract quantities of interests, e.g. QSS rate coefficients,

$$\frac{\partial n_c^i}{\partial t} = \omega_c^i, \tag{1}$$

where ω_c^i is the production term.

Master Equation (2)

Consider the generic heterogeneous exchange reactions,

$$\mathrm{AB}_i + \mathrm{C}_j \underset{k^{\mathrm{AB}_i-\mathrm{C}_j}_{\mathrm{AC}_m-\mathrm{B}_n}}{\overset{k^{\mathrm{AC}_m-\mathrm{B}_n}_{\mathrm{AB}_i-\mathrm{C}_j}}{\rightleftharpoons}} \mathrm{AC}_m + \mathrm{B}_n \qquad \text{(Reaction 5)}$$

The production term is given by,

$$\omega^i_{\mathrm{AB}} = -\left[k^{\mathrm{AC}_m-\mathrm{B}_n}_{\mathrm{AB}_i-\mathrm{C}_j} n^i_{\mathrm{AB}} n^j_{\mathrm{C}} - k^{\mathrm{AB}_i-\mathrm{C}_j}_{\mathrm{AC}_m-\mathrm{B}_n} n^m_{\mathrm{AC}} n^n_{\mathrm{B}}\right], \qquad (2)$$

where forward, i.e. $k^{\mathrm{AC}_m-\mathrm{B}_n}_{\mathrm{AB}_i-\mathrm{C}_j}$, and reverse, i.e. $k^{\mathrm{AB}_i-\mathrm{C}_j}_{\mathrm{AC}_m-\mathrm{B}_n}$, rate coefficients are related by the equilibrium constant,

$$K_{eq} = \frac{k^{\mathrm{AC}_m-\mathrm{B}_n}_{\mathrm{AB}_i-\mathrm{C}_j}}{k^{\mathrm{AB}_i-\mathrm{C}_j}_{\mathrm{AC}_m-\mathrm{B}_n}} = \frac{g^i_{\mathrm{AB}} g^j_{\mathrm{C}} Q^t_{\mathrm{AB}} Q^t_{\mathrm{C}}}{g^m_{\mathrm{AC}} g^n_{\mathrm{B}} Q^t_{\mathrm{AC}} Q^t_{\mathrm{B}}} e^{\frac{E^m_{\mathrm{AC}}+E^n_{\mathrm{B}}-E^i_{\mathrm{AB}}-E^j_{\mathrm{C}}}{k_B T}}, \qquad (3)$$

where Q^t is the unit-volume translational partition function.

Master Equation (3)

Methodology

For inelastic and dissociation processes,

- Endothermic processes are considered due to better sampling properties,
- Exothermic rate coefficients are reconstructed by imposing the principle of detailed balance.

For heterogenous exchange processes,

- Exothermic processes are considered due to better sampling properties,
- Endothermic rate coefficients are reconstructed by imposing the principle of detailed balance.

Master equations are numerically integrated using `PLAsma in Thermodynamic nOn-equilibrium` (`PLATO`) library developed within the Center for Hypersonic Entry System Studies (CHESS) at the University of Illinois Urbana Champaign.

Master Equation (4)

Numerical Setup

- Isothermal and isochoric reactor initialised with n $= 2.4\ 10^{23} \mathrm{m}^{-3}$ (P = 1000 Pa and $T_0 = 300$ K) with species mole fractions $\chi_{\mathrm{NO}} = 0.5$ and $\chi_{\mathrm{C}} = 0.5$,
- Reactor is plunged in heat baths maintained constant throughout the numerical experiments, i.e. $T_{\mathrm{bath}} = 7500$, 10000, and 20000 K,
- The translational mode is distributed according to the Maxwell-Boltzmann distribution at T_{bath}, and the internal modes are distributed according to the Boltzmann distribution at T_0,
- Rovibrational dissociation, and exchange processes studied sequentially,
- Ionisation and charged species are disregarded.

Outline

Dissociation Processes

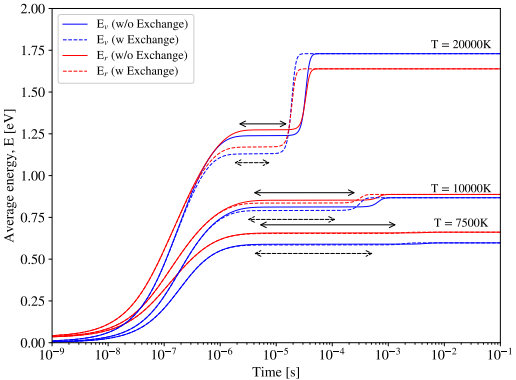

Figure: Average rotational and vibrational energy distribution of NO at three different kinetic temperatures (heterogeneous exchange processes excluded). The arrows indicate the QSS periods. The solid arrows denote the QSS for the direct dissociation, and the dashed arrows denote the QSS for the total dissociation.

Dissociation Processes

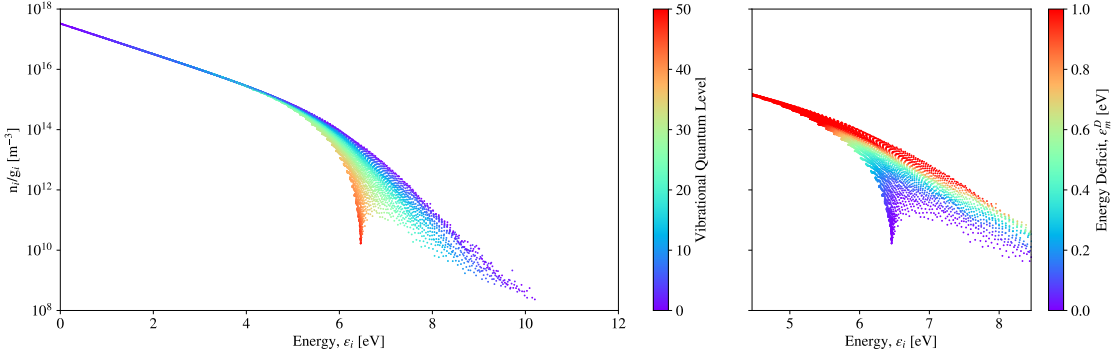

Figure: Rovibrational distribution amid the QSS region at T = 10,000 K (heterogeneous exchange processes excluded). The distributions are coloured by the vibrational quantum number and energy deficit.

Dissociation Processes

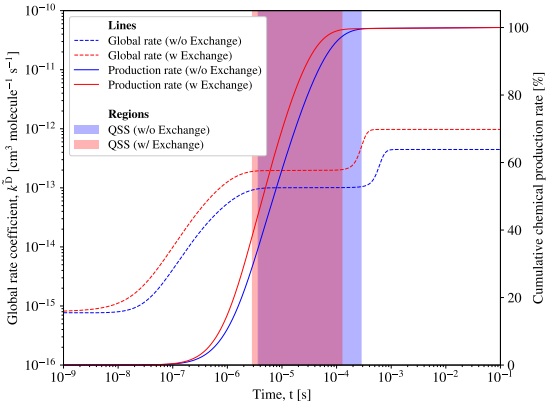

Figure: Time cumulative chemical production and global dissociation rate of $NO(X^2\Pi_r) + C(^3P)$ at T = 10,000 K (heterogeneous exchange processes excluded).

Exchange Processes

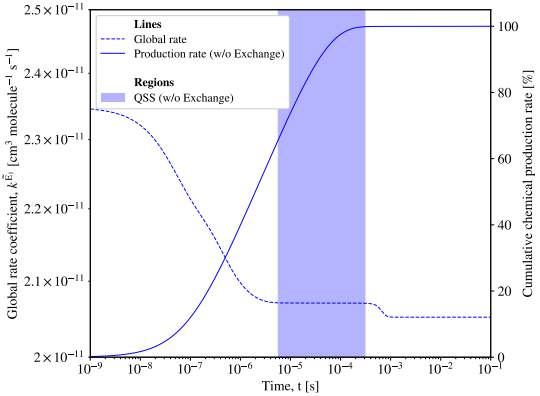

Figure: Time cumulative chemical production rate coefficient of $NO(X^2\Pi_r) + C(^3P) \longrightarrow CN(X^2\Sigma^+) + O(^3P)$ at T = 10,000 K (dissociation processes included). The solid arrows denote the QSS for the direct dissociation.

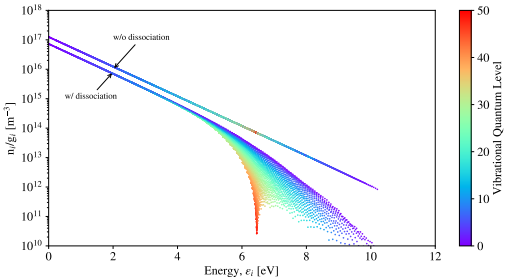

Figure: Rovibrational distribution of NO at t = 1.35 10^{-4} s and T = 10,000 K with and without dissociation kinetics. The inital mole fraction is set to $\chi_{NO} = \chi_C = 0.5$.

Exchange Processes

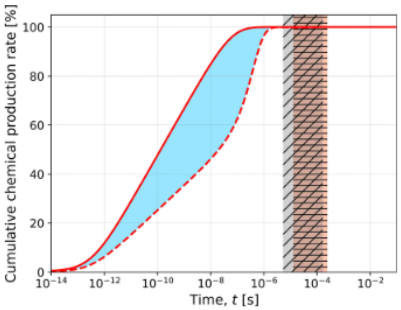

Figure: Time cumulative chemical production rate coefficient of $N_2 + O \longrightarrow NO + N$ at T = 10,000 K. The cyan-shaded areas represent the region where the chemical reaction occurs. The red lines indicate the two different limiting cases of initial mole fractions. The figures share the plot legend. (extracted from Jo *et al* (2022))

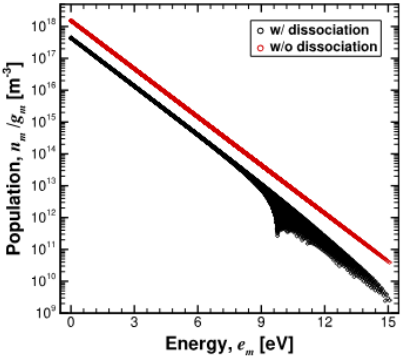

Figure: Rovibrational distribution of N_2 for $N_2 + O \longrightarrow NO + N$ at t = 4.0 10^{-5} s and T = 10,000 K with and without dissociation kinetics. The inital mole fraction is set to $\chi_{N_2} = \chi_O = 0.5$. (extracted from Jo *et al* (2022))

Thermal Rates

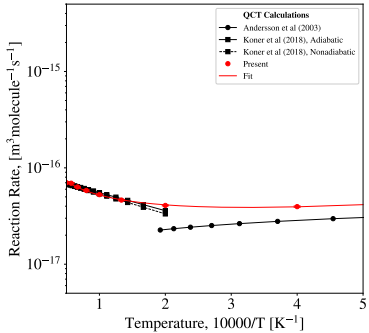

(a) $NO(X^2\Pi) + C(^3P) \longrightarrow CN(X^2\Sigma^+) + O(^3P)$.

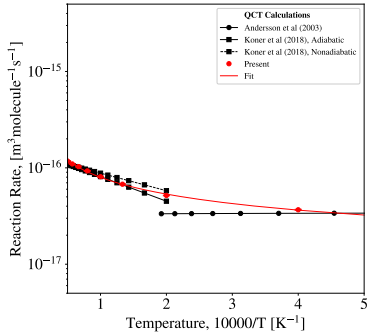

(b) $NO(X^2\Pi) + C(^3P) \longrightarrow CO(X^1\Sigma^+) + N(^4S, ^2D)$.

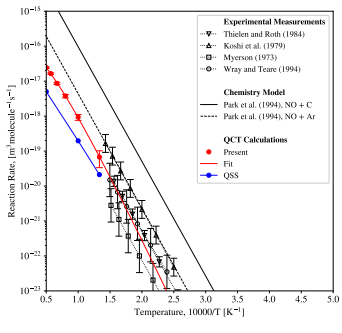

(c) $NO(X^2\Pi) + C(^3P) \longrightarrow N(^4S) + O(^3P) + C(^3P)$.

Figure: Comparison of the thermal exchange rates of the three exothermic exchange reactions and dissociation reaction of $NO(X^2\Pi_r) + C(^3P)$ against experiments and QCT calculations.

Outline

Conclusions

- **Inelastic processes:**
  - low lying states proceed through rotational excitation by conserving the initial vibrational quantum level,
  - high lying states transfer energy through rovibrational excitation.
- **Dissociation processes:**
  - rovibrational state-specific rate coefficients governed by exchange-assisted mechanisms (similarities with HCN (Sharma *et al* 2022)),
  - rovibrational distribution of high lying states are highly correlated to the levels' energy deficit (similarities with O_3 (Venturi *et al* 2020) and N_2O (Jo *et al* 2022)).
- **Exchange processes:**
  - no QSS condition reached without dissociation kinetics (similarities with N_2O (Jo *et al* 2022)),
  - invalidate the QSS approximation adopted when modelling chemical reactions in hypersonic CFD codes, e.g. Zel'dovich.
- Thermal and QSS rate coefficients in good agreement with experiments and theoretical studies.

Perspectives

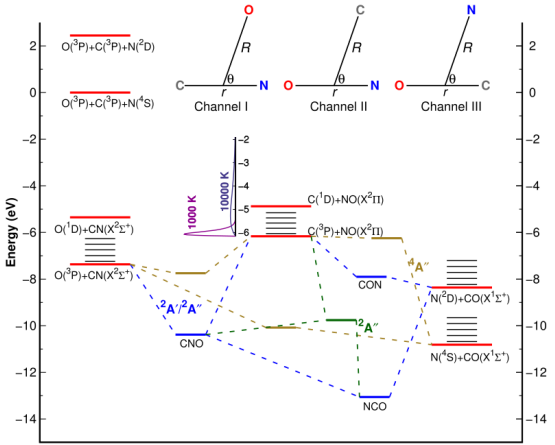

Figure: Schematic of the energy profile for the CNO system. (Extracted from Koner *et al.* (2018))

Thank you for your attention!

C. H. B. Civrais[1], B. R. L. Galvão[2], S. M. Jo[3], M. Panesi[1]

[1]Department of Mechanical and Aerospace Engineering, University of California Irvine, Irvine, USA
[2]Centro Federal de Educação Tecnológica de Minas Gerais, Belo Horizonte, Minas Gerais, Brazil
[3]Korea Advanced Institute of Science and Technology, Republic of Korea

Thermal & Fluids Analysis Workshop 2025
NASA Ames Research Center
San Jose, CA
August 4-7, 2025

Thermal Rates

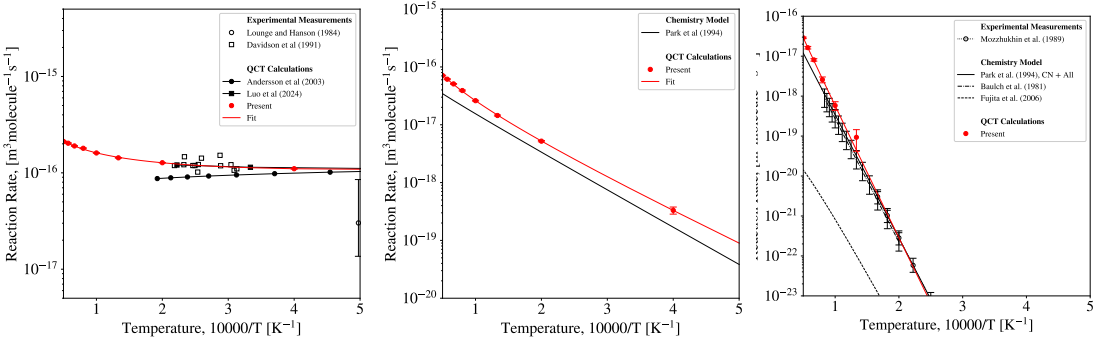

(a) $CN(X^2\Sigma^+) + O(^3P) \longrightarrow CO(X^1\Sigma^+) + N(^4S, ^2D)$.

(b) $CN(X^2\Sigma^+) + O(^3P) \longrightarrow NO(X^2\Pi) + C(^3P)$.

(c) $CN(X^2\Sigma^+) + O(^3P) \longrightarrow C(^3P) + N(^4S) + O(^3P)$.

Figure: Comparison of the thermal exchange and dissociation rate coefficients of $CN(X^2\Sigma^+) + O(^3P)$ against experiments and QCT calculations.

Thermal Rates

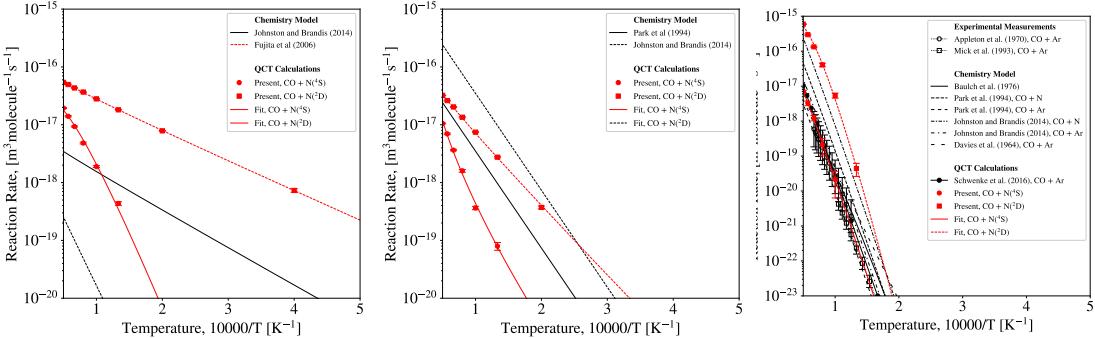

(a) $CO(X^1\Sigma^+) + N(^4S, ^2D) \longrightarrow NO(X^2\Pi) + C(^3P)$.

(b) $CO(X^1\Sigma^+) + N(^4S, ^2D) \longrightarrow CN(X^2\Sigma^+) + O(^3P)$.

(c) $CO(X^1\Sigma^+) + N(^4S, ^2D) \longrightarrow C(^3P) + O(^3P) + N(^4S)$.

Figure: Comparison of the thermal exchange and dissociation rate coefficients of $CO(X^1\Sigma^+) + N(^4S, ^2D)$ against experiments and QCT calculations.